LANGMUIR Article
Cite This: Langmuir 2019, 35, 8977−8983
pubs.acs.org/Langmuir

Dynamical Clustering and Band Formation of Particles in a Marangoni Vortexing Droplet

Ashish Kumar Thokchom[†] and Sehyun Shin*[,†,‡]

[†]Engineering Research Center for Biofluid Biopsy and [‡]School of Mechanical Engineering, Korea University, Seoul 02841, Republic of Korea

Supporting Information

ABSTRACT: Drying a droplet containing microparticles results in the deposition of particles in various patterns, including the so-called "coffee-ring" pattern. The particle deposition is dependent on the internal flow dynamics, such as the capillary flow and Marangoni vortex (MV), of the droplet. Particle migration and self-assembly on a substrate are interesting phenomena that have critical implications in many applications such as inkjet printing, coating, and many other droplet-based industrial processes. In this work, we observed the formation of bands of particles in a rotating MV during the evaporation of a water droplet containing particles. We investigated the mechanism underlying the formation of banded MV caused by capillary meniscus forces between two particles near the air−liquid interface. In particular, we show that the banded MV can be manipulated by tuning the surfactant concentration and particle concentration. Our findings would provide a new direction in understanding the particle deposition pattern of a colloidal droplet.

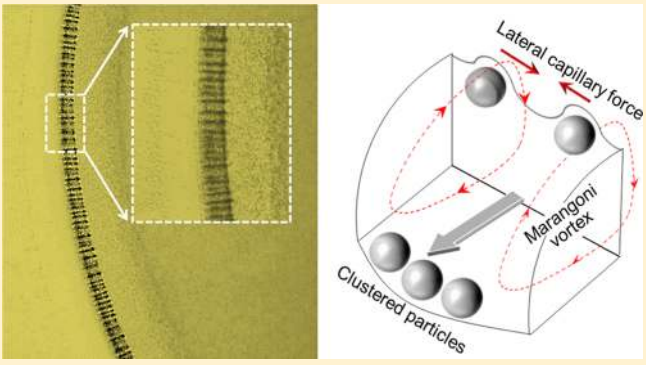

INTRODUCTION

Most drying droplets with a pinned contact line leave particle near the edge-like ring structure after the complete evaporation of the solvent. This is considered to be a kind of self-assembly of particles caused by the radial outward flow of solvent from the center to the edge of the droplet, which is commonly known as the coffee ring effect.[1] It has been found that the existence of motion of the fluid flow known as Marangoni flow driven by surface tension gradient can alter particle transport and suppress the coffee ring phenomenon during the evaporation process.[2−5] Scientists working across fields ranging from fundamental science to industry have paid tremendous attention to control this phenomenon. Controlling particle deposition on substrate from an evaporating droplet has a great impact in many applications such as coating,[6] micro-/nanofabrication,[7] point-of-care medical diagnosis,[8,9] and modern inkjet printing.[10,11] This seemingly simple phenomenon is a complex process involving many factors such as dynamics of the contact line,[12] atmospheric condition,[13] and substrate−particle[14] or particle−particle interactions.[15,16] Most methods used to control the particle deposition from an evaporating droplet involve modifying the surface wettability,[17] mediating the surfactant in the solution,[18] changing the shape of the particle,[19,20] solvents,[21] external heating of the substrate,[22] and so forth.

For instance, interaction between particle−particle or particle−substrate can be manipulated by controlling the pH value of a droplet solution, which results in changes of Derjaguin−Landau−Verwey−Overbeek (DLVO) interaction. At low pH (pH ≈ 1.5), particle−substrate attractive interactions promote particle adhesion at the substrate and eventually lead to a homogeneous deposit, whereas at high pH, particle−substrate interactions are repulsive, and particles are collected to the contact line with forming a ring-shaped pattern.[15,23] In fact, there are diverse interactions involving particles and interfaces including Coulomb and van der Waals interactions, capillary forces, and hydrophobic interactions. These interactions are generally strong and affect particle organization and behavior at interfaces.[25]

When a surfactant-like polymer is added in a droplet solution, the particle deposition is strongly influenced by the concentration and molecular weight of the surfactant dissolved into the solution. Evaporation of drops of both low and high concentrations of polymer into solution showed a ring-like pattern after drying, while the drops of intermediate concentration of surfactant into the solution show a uniform deposition on the substrate.[23] Furthermore, colloidal drop shows multiple ring deposition on the substrate after complete evaporation.[24] This is due to the competition between the receding contact line and particle deposition during the evaporation of the droplet. This pattern formation is also dependent on the particle size dispersed into the solution.

Received: March 23, 2019
Revised: May 16, 2019
Published: June 12, 2019

Small particles show a multiple ring deposition while the larger particles suppress the multiple ring formation.[25]

Interestingly, there are some reports on the spatial ordering of particles in a drying droplet. When a bidisperse colloidal mixture consisting of microparticles and nanoparticles is suspended in a droplet, fingering is formed inside the coffee ring because of the competition between the coffee-ring and Marangoni effects, especially when the inward Marangoni flow is overwhelmed by the outward coffee-ring flow.[26] A similar spatial ordering was also observed in a drying polymer solution with suspended particles.[27] This phenomenon was attributed to the combination of phase separation of bridged particles and the Marangoni flow effect. Although this phenomenon is still not fully understood, Marangoni flow has been suggested to be a potential parameter causing the spatial ordering of particles. In our previous study, we comprehensively considered the Marangoni vortex (MV) driven by the surface tension gradient[18] and observed a similar phenomenon, which we did not report. In the present work, we investigated the formation of particle bands in an evaporating droplet. The main objective is to delineate the mechanism of particle clustering dynamics and band formation of particles in an evaporating droplet by systematically varying the MV strength and particle concentration.

MATERIALS AND METHODS

Materials. Polyethylene glycol (PEG; MW = 35 000) used as the surfactant was purchased from Sigma-Aldrich, Korea (www.sigmaaldrich.com). Glass slides (Lauda-Königshofen, Germany) were used as the substrate.

Preparation of the Particle Suspension. First, we prepared a solution of PEG in deionized (DI) water. Different amounts of PEG powder were dissolved in DI water to obtain 0.3, 0.75, and 3 wt % of PEG in water, and these solutions were used for the experiments. Further, we used 1 μm polystyrene particles (Thermo Fisher Scientific, MA, USA). The suspension of the particles was centrifuged at 4000 rpm for 5 min, and the recovered particles were resuspended in the aforementioned PEG solutions. The suspensions were shaken well to disperse the aggregated particles. Different amounts of the particles were suspended in 0.75 wt % PEG solution to obtain final particle concentrations of 0.5, 1, 2, and 5 wt %. To study the effect of the size of the particles, we used 0.5 and 5 μm polystyrene particles (Thermo Fisher Scientific, MA, USA) in the experiments. The entire experiment was performed in an enclosed room where the temperature and humidity were maintained at 23 ± 1 °C and 20 ± 3% RH, respectively.

Analyses of Particles and Final Deposition Patterns after the Evaporation of the Droplet. We used an optical microscope mounted with a camera (IX71 Olympus Co., Japan) to observe the particles and pattern formation. The images of the particles inside the droplet were captured at the frame rate of 30 fps. The inverted grayscale intensity of the captured images was measured using the ImageJ software.

RESULTS

Formation of Bands of Particles during the Evaporation. Figure 1 summarizes the formation of particle bands inside the MV during the evaporation of a water droplet containing polystyrene spheres. To investigate this phenomenon, a 2 μL water droplet containing 1 μm diameter polystyrene particles suspended at 2 wt % weight concentration was placed on a glass substrate. The particles inside the droplet were monitored at various time intervals using an optical microscope at room temperature. Figure 1a illustrates the layout of our experimental setup. Radial outward flow of the fluid from the center to the edge of the water droplet was observed. Addition of a surfactant-like polymer, PEG, to water drastically changed the internal flow dynamics and the particle distribution in the evaporating droplet.

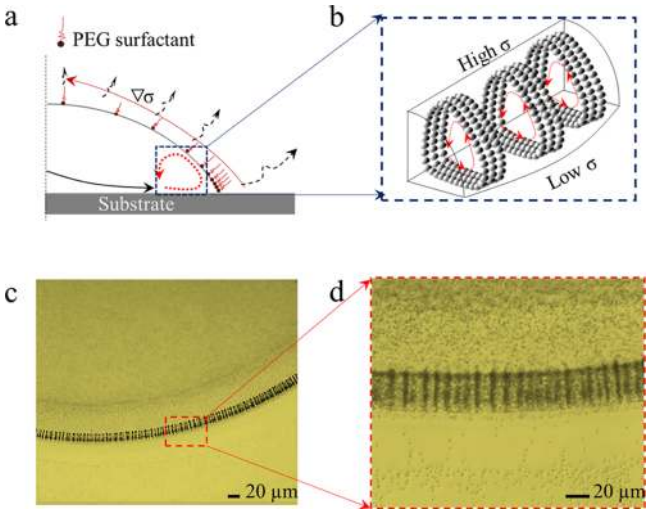

Figure 1. Summary of the banded MV inside the evaporating droplet. (a) Illustration of the internal fluid motion in a droplet of PEG−water solution. (b) Schematic of a banded MV in an evaporating droplet. (c,d) Snapshots of a banded MV in the evaporating droplet placed on a glass substrate.

In the early stage of the evaporation process, the radial outward flow of water transports particles as well as the PEG polymer to the edge of the droplet. As time progresses, an inward flow, the so-called Marangoni flow, is generated inside the evaporating droplet. In our previous study, we have previously confirmed that the surfactant-like polymer of PEG is highly concentrated near the edge because of the outward capillary flow.[18] Typical values of the surface tension were 58.5 dyne/cm near an edge and 59.5 dyne/cm at the bulk region. As a result, surface tension which is a function of distribution of PEG surfactant is lower at the edge than at the other region of the droplet. This creates a Marangoni flow driven by surface tension gradient from the region of lower surface tension to the higher surface tension region along the air−liquid interface of the droplet. The profiles of PEG concentration and surface tension near the edge were fully described in our previous study.[18] Subsequently, these two opposite directional flows are connected and a closed-loop flow is formed, which is the so-called "MV," as shown in Figure 1b. The PEG polymer not only acts as a surfactant but also increases the viscosity of the suspension; concentrated PEG induces a stable vortex with time. This clear evident can be seen from the recorded video files provided in the Supporting Information (Video S1).

While particles move along the streamlines of the MV, monodisperse particles tend to gather and form multiple bands of particles (Video S2). As time progresses, the formation of particle bands becomes apparent in the rotating vortex. Interestingly, the structure and pattern of multiple bands are regular and periodic, respectively. In fact, after the evaporation of the droplet, multiple bands existing in the rotating flow lead to spatial ordering of particles (Figure 1c,d).

The evolution of the banded MV inside the evaporating droplet is worth noting (Figure 2a). When an MV is generated in the evaporating droplet, particles tend to aggregate and form bands of particles with it at time t = 20 s. (particle diameter

DOI: 10.1021/acs.langmuir.9b00865
Langmuir 2019, 35, 8977−8983

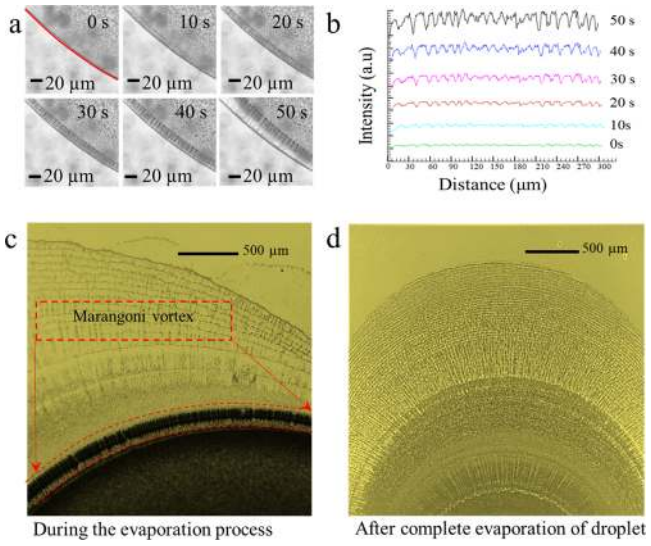

Figure 2. Time evolution of the banded MV during the evaporation of a droplet. (a) Captured images showing the evolution of a banded MV during the evaporation of a droplet containing 2 wt % particles suspended in a 0.75 wt % PEG solution. (b) Grayscale intensity plot at various time intervals of the evaporating droplet. (c) Captured image of the banded MV and particle pattern formed on the substrate during the evaporation process. (d) Final pattern formation after complete evaporation of the solvent.

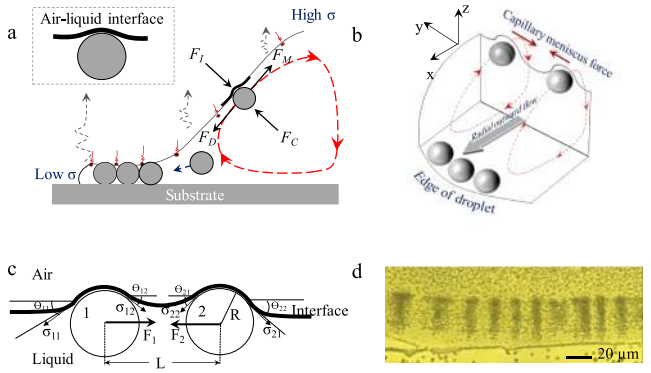

Figure 3. Mechanism of the formation of a banded MV inside the evaporating droplet. (a) Various forces acting on the particle suspended in the evaporating droplet. (b) Representation of CMFs between two particles within the MV during the evaporation process. (c) Schematic of CMFs between two particles at the air−liquid interface. (d) Captured image of a banded MV inside the evaporating droplet.

(d_p) = 1 μm, particle concentration (ϕ_p) = 2 wt %, PEG concentration (ϕ_{PEG}) = 0.75 wt %). As time progresses, well-ordered and periodic bands of particles are formed and the band peak intensity increases. The most apparent bands are observed at t = 40 and 50 s, with a typical spacing of 10−15 μm (Figure 2a).

We further characterized the formation of a banded MV during the droplet evaporation by measuring the inverted grayscale intensity, as represented in Figure 2b. The amplitude of the measured intensity increased with time as the particle clustering is progressed. Similar to the photographs of Figure 2a, the maximum amplitude was observed at t = 50 s. It is worthy to note that the number of radial bands do not change in the initial time zone (t < 50 s), as shown in Figure 2b. For t > 50, the band peak intensity decreases with time and the number of radial bands also changes with time (not shown). The changes in the number of bands and peak intensity may be due to the changes of internal flow with decreasing contact angle, which sweeps away particles from the banded ones. Thus, subsequently, the spacing between the bands is reduced and the sharpness of the bands is also reduced. During the evaporation, the edge line depinned, moves inward, and pins again with the formation of the MV (Figure 2c). When the edge moves inward, particle−substrate interaction would determine deposition patterns, as shown in Figure 2c,d. After complete evaporation of the droplet, the final deposition of the particles on the substrate in a fingerprint-like pattern is observed (Figure 2d). Various final deposition patterns are depicted in Figure S1.

Mechanism of the Generation of Banded MVs. Figure 3a−d illustrates the underlying mechanism of formation of particle bands during the evaporation of a droplet of the particle suspension placed on a glass substrate. Particles at the droplet edge are exposed to the air−liquid−substrate interface in the dotted box of Figure 3a. Considering a moving particle located at the air−liquid interface, various forces act on the particle, including the centrifugal force (F_C), interfacial tension force (F_I), Marangoni force (F_M), and drag force (F_D). The Marangoni flow driven from the lower region of surface tension to the higher region of surface tension created by the surface distribution of PEG surfactant will create the Marangoni force (F_M) on the particle. The Marangoni force is $F_M = \Delta\sigma l$, where $\Delta\sigma$ is the surface tension gradient and l is a length of MV. F_D denotes the drag force ($6\pi\mu DV$), which can impede the motion of the particle in the Marangoni flow. Here, μ is the viscosity of liquid, D is the diameter of a particle, and V is the velocity of particle. The particle which rotate along with the motion of MV experiences the centrifugal force ($F_C = \pi D^2\rho V^2/3$). F_I is the interfacial force acting on the particle ($F_I = \pi D\sigma$). Because the particles are neutrally buoyant, the effect of gravity is negligible. Though a rough estimate of these forces, the centrifugal force was found to be small compared to others.

Even though Figure 3 described dynamics of particles located near the air−liquid interface, particles rotating in inner orbits would not meet the air−liquid interface. When a strong capillary flow drives particles near the edge of a droplet, then particles may reach the outer orbit near the air−liquid interface. Also, while the particles turn the direction of motion, the centrifugal force may exert on particles and drives outer orbits. However, rough estimate of the centrifugal force was found to be too small to change particles' orbits. When the particles reached the interface, each individual particle will cause perturbation in the shape of liquid interface or film at the free liquid surface as shown in the inset picture of Figure 3b. Once the perturbation around the particles overlapped, it causes imbalance in the capillary meniscus forces (CMFs) that arise from different curvatures of the air−liquid interface due to the particles as shown in Figure 3c. This force is strong enough to cause the 2D dimensional structures and ordering of particles in many experiments.[28−31] When the interparticle distance is relatively short, particle−particle attraction occurs and multiple bands of particles become apparent in the MV. One of the interesting facts is that once the particles aggregate, it remains as a group even into the bulk of the fluid. This may arise from the van der Waals forces between the particles.[15,23]

DOI: 10.1021/acs.langmuir.9b00865
Langmuir 2019, 35, 8977−8983

The lateral translational motion of the particles is caused by the imbalanced CMFs acting between the particles at the air−liquid interface, as shown in Figure 3c. If the interparticle distance is large, the neighboring particle does not interfere with the air−liquid interface line, and thus the CMFs around a particle are symmetric (i.e., $\sigma_{11} = \sigma_{12}$) and this particle would not attract neighboring particles. When the particles are close enough, the overlapped interfacial shape around the particles causes imbalance in the CMFs, which is caused by the different curvatures of the air−liquid interface between the left and right sides of the particle. As a result, the neighboring particles attract each other and recruit other neighboring particles in the same manner. Subsequently, monodisperse particles in a droplet aggregate and form multiple bands of particles in the MV, as shown in Figure 3d and Video S2. After the droplet evaporates, an intermittent coffee ring effect is produced, as shown in Figure 1d.

Control of the Formation of Particle Bands: Strength of MV. As described above, the MV is a prerequisite for the formation of bands of particles. To examine the effect of the strength of MV on the formation of bands of particles, we conducted experiments with three different concentrations of PEG in the solution (0.3, 0.75, and 3 wt %). The concentration of the polystyrene particles (d_p = 1 μm) in the solution was fixed at 2 wt % in these experiments. For the lowest concentration of the PEG solution (0.3 wt %), a weak MV was generated for a short time, but no apparent formation of bands of particles was observed in the droplet (Figure 4a). For the 0.75 wt % PEG solution, the MV was generated near the edge of the droplet right from the beginning. Rotating particles gathered gradually and formed bands of particles within the MV of the evaporating droplet (Figure 4b). Meanwhile, for the highest concentration (3 wt %) of the PEG solution, a strong MV formed in terms of the vortex velocity as well as the vortex size. However, there were no apparent bands of particles inside the droplet, as shown in Figure 4c.

When the particle concentration was increased further to 5 wt %, formation of particle bands became apparent (Figure 4d). It is worthy to note that in Figure 4c,d, the concentration of PEG (3%) is the same, but the particle concentration is different. When the particle concentration increases, the local viscosity of the suspension near the droplet edge is significantly increased due to the coffee-ring effect. Thus, 3% of PEG solution for a 2 wt % particle concentration showed a strong MV but not for 5 wt % particle concentration as shown in Figure 4d. Thus, we found that the generation of MV is solely dependent on the PEG concentration but suspension viscosity depending on particle concentration also affects the strength of MV. These results are compared in the Supporting Information (Video S3).

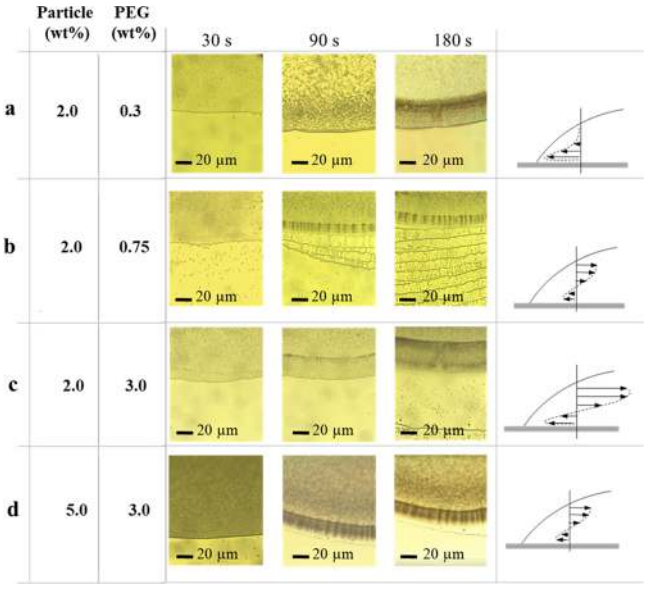

Figure 4. Effect of the PEG concentration on the banded MV inside the evaporating droplet. Schematic illustrations of various velocity profiles inside an evaporating droplet and corresponding layouts of the motion of the fluid flow inside the evaporating droplet. (a−c) Captured images of a droplet containing 2 wt % particles suspended in (a) 0.3, (b) 0.75, and (c) 3.0 wt % PEG solution recorded at 30, 90, and 180 s. (d) Captured images of a droplet containing 5 wt % particles in a 3 wt % PEG solution recorded at 30, 90, and 180 s.

Controlling the Formation of Particle Bands: Particle Concentration. To further analyze the observed phenomenon, we investigated the effect of the particle concentration on the formation of bands of particles inside the droplet. We conducted the experiments with suspensions of four different particle concentrations, viz., 0.5, 1, 2, and 5 wt %, dispersed in a 0.75 wt % PEG solution. Figure 5 shows the images of evaporating droplets with varying particle concentrations. At 0.5 wt % particles in the suspension, there is no formation of bands of particles in the droplet during the process (Figure 5a); however, there are small clusters in the rotating MV (Video S4). In case of suspensions with 1 and 2 wt % particles, the particles undergo self-aggregation and particle bands are formed in the droplet. At a fixed PEG concentration (0.75 wt %), the droplet with 2 wt % particles shows the formation of multiple bands of particles at a faster rate than that observed in the case of a droplet with 1 wt % particles. However, the bands of particles did not form clearly when the particle concentration was increased to 5 wt %. The obtained results can be better understood from the video files provided in the Supporting Information (Video S4).

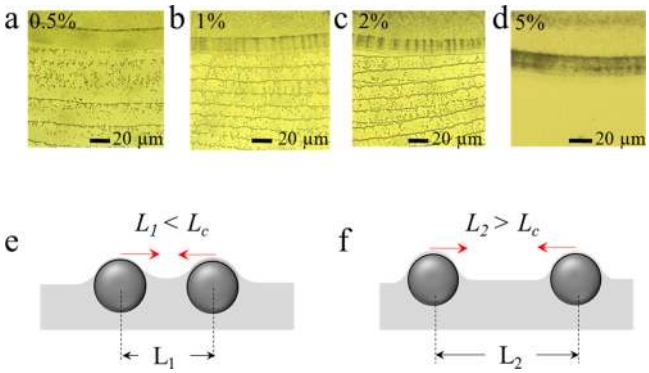

Figure 5. Effect of the particle concentration on the banded MV inside the evaporating droplet. The obtained images of the droplet containing different concentrations of the particles: (a) 0.5, (b) 1, (c) 2, and (d) 5 wt % suspended in a 0.75 wt % PEG solution. Schematic of the particle-to-particle distance and the corresponding CMFs between them (e) $L_1 < L_c$ and (f) $L_2 > L_c$.

The particle concentration is directly related to the interparticle distance. Because the distance between the particles (L_1) is within an effective range (L_c) of the CMFs acting between the particles attached to the air−liquid

DOI: 10.1021/acs.langmuir.9b00865
Langmuir 2019, 35, 8977−8983

interface, the particles easily attract each other and aggregate, as shown in Figure 5e. When $L_2 < L_c$, the CMFs acting on a particle are not perturbed by the neighboring particles, and they do not induce self-aggregation of particles, as depicted in Figure 5f.

DISCUSSION

Dynamics of Particle Clustering. The formation of particle bands is directly associated with the MV. Through the present study, we found that the formation of multiple bands of particles during the evaporation requires an essential condition of imbalanced lateral capillary forces between the particles. This condition would be satisfied with a moderate strength of the MV as well as an effective interparticle distance. The former condition puts particles at the air−liquid interface, wherein the CMFs can work. The latter condition breaks the symmetric CMFs acting on a particle due to the overlapped perturbed interfaces. Thus, particle band formation in an evaporating droplet should be accompanied with the MV, as well as imbalanced CMFs.

A similar kind of particle dynamics can be found in a rotating cylinder with partially filled liquid.[32−34] When the cylinder rotates continuously at a constant velocity, the completely wet particles gradually segregate with time after passing through a few stages. Initially, the particles associate into many small particle clusters that subsequently merge into larger ones. Eventually, they form cylindrical bands. Both MV system and partially filled rotating cylinder form particle clustering with similar mechanisms. First, both systems hold the air−liquid interface, in which CMF can be effective to attract particles. Second, both system hold rotating flow, which transport suspended particles to the air−liquid interface. Finally, the lateral CMF is the main force for particles to aggregate and to form banded particles in both systems. Even though these dynamic similarities should be further analyzed, both systems form similar banded particles.

Effective Length of CMFs. The effective distance of CMFs is known to be several folds the particle diameter.[26] As described above, CMFs between the particles are strongly influenced by the particle concentration in the suspension. Assuming an appropriate MV, particles can flow along or near the air−liquid interface. As shown in Figure 5a, at a low concentration of 0.5 wt %, the particles did not associate to form particle bands, which might be due to the large interparticle distance. Considering that the formation of particle bands is caused by the lateral motion of particles associated with the CMFs, the lateral distance between the particles should be considered rather than the front and rear distance between particles. In fact, the interparticle distances seem to be short in Figure 5a, but the lateral distance between particles may not be within the effective length of the CMFs. With increasing particle concentration, the interparticle distance would be decreased, and indeed, bands of particles were observed. Moreover, the CMFs are strong enough to generate regular 2D dimensional structures and induce ordering of particles.[26−29] Thus, once the particles are within the effective distance of the CMFs, they will be attracted to each other to form clusters, eventually leading to multiple bands of particles.

Effect of the Particle Size. Note that the CMFs are dependent on the size of the particle.[26,28] We conducted additional experiments with particles of different sizes, 0.5, 2, and 5 μm (not shown), of 2% were dispersed into 0.75 wt %. We conducted additional experiments with particles of different sizes, 0.5, 2, and 5 μm (not shown), while fixing the concentrations of the particles and PEG at 2 and 0.75 wt %, respectively. Considering that the generation of MV is solely dependent on the PEG concentration, the MV exists whether or not the particles experience the MV. For the smallest particles (0.5 μm), there was no formation of particle bands even though the MV exists. However, the reference particles (2 μm) formed apparent bands of particles. In fact, the MV velocity for 0.5 μm particles was found to be relatively faster than that for 2 μm. There may be two factors to prevent the 0.5 μm particles from forming bands: one is the excessive speed of particles in the Marangoni flow and the other is the influence of the particle size on the CMFs. The captured images were provided in the Supporting Information as the Figure S2.

In the present study, it is seemed that the larger the particles are, the stronger the CMFs are. Considering the cubic function of particle volume to diameter, one could raise a question that the number of particles for bigger ones will be much smaller for the same weight % suspensions and a normalized parameter, d/L ratio (particle diameter/particle−particle distance), may be considered as the true parameter rather than the actual particle size. This consideration may be right in a stationary flow environment. However, when capillary flow in a droplet transports particle toward edge and the sparsely distributed particles are getting dense near the edge, the ratio of d/L may not be meaningful any longer. As the interparticle gradually distance decreases, larger particles begin to aggregate earlier than smaller particles. Thus, in the present results, the particle size would be more directly effective on the particle clustering rather than the relative one such as d/L.

For investigating the former issue, we need to revisit the Marangoni number, $\mathrm{Ma} = \Delta\sigma l/6\pi\mu DV$, which delineates the Marangoni flow phenomenon.[18] Here, $\Delta\sigma$, l, μ, D, and V denote the surface tension gradient, size of the MV, solution viscosity, particle diameter, and particle velocity, respectively. Because the viscous drag ($F = 6\pi\mu DV$) is proportional to the particle diameter, small particles would have higher velocity than large particles, which may reduce the interaction time of CMFs between the particles. In addition, such an excessive velocity would perturb the air−liquid interface near the particles and the imbalanced CMFs would be weakened. Second, the magnitude of CMFs as well as the effective distance of CMFs is directly related to the size of the particles. The smaller the particles are, the weaker the CMFs would be[26,28] and the shorter the effective distance of CMFs is. Consequently, small particles lead to increased Marangoni velocity and imbalanced CMFs, which prevent the formation of bands of particles in the MV.

As demonstrated in Figure 4c,d, with a fixed PEG concentration (ϕ_{PEG} = 3 wt %), there was a strong MV but no particle band formation for a relatively low concentration of particles (ϕ_p = 2 wt %), whereas there was a moderate MV and apparent particle band formation for a relatively high concentration of particles (ϕ_p = 5 wt %). These results may be associated with the Marangoni flow velocity along the air−liquid interface. If particles move rapidly along the interface, the interfacial shape would be widely and strongly perturbed and thus the imbalanced effect of CMFs would be weakened. When the particle concentration is increased, the viscosity of the suspension increases, and thus the corresponding

DOI: 10.1021/acs.langmuir.9b00865
Langmuir 2019, 35, 8977−8983

Marangoni velocity decreases. For clarification, the sketches of velocity profiles are provided in Figure 4e,f.

Effect of Electrostatic and van der Waals Forces. The dynamics of particle clustering in a MV was delineated with the lateral translational motion of the particles caused by the lateral capillary force.[36] Because the particle clustering may be affected by particle aggregation, it is necessary to examine the effect of DLVO interaction on the particle aggregation.[15] First, there were no apparent changes in pH values by adding PEG in DI water. The pH value of DI water was 7.0, whereas that of 0.75% PEG solution was 7.3. Even for considering concentrated PEG solution near the edge of a droplet, it is still lower than 7.8 because the used PEG is non-ionic polymer. Second, the zeta potential of PS microparticles in the PEG solution was found to be small. A previous study reported that when PEG was adsorbed on polystyrene particles, its zeta potential was significantly decreased from −59 to −1 mV.[35] Thus, the effect of DLVO interaction on particle aggregation would be negligibly small.

We have considered formation of banded particles near the air−liquid interface by the CMF, which would be dominant over other forces. It is worthy to note that when the banded particles transport back to the bulk of the droplet, CMF disappears and other forces would be a new dominant one. If the particles are strongly charged, then repulsive electrostatic forces would destroy the banded particles. Because the zeta potential of particles was small, there would not be any significant repulsive electrostatic force or attractive van der Waals force between particles. Thus, van der Waals force may hold the banded particles together while the capillary interaction disappears in a bulk fluid region of MV.

It would be more interesting to extend our study to microparticles with a different aspect ratio dispersed in the surfactant solution. Studies on periodic bands of particles in a coffee ring might provide better insights on the mechanism of the self-assembly of nanoparticles during the evaporation of droplets of various colloidal suspensions. Moreover, controlling the particle deposition pattern formed from a drying droplet has a great impact on the assembly of well-ordered micro-/nanoparticle structures on various substrates for fabricating artificial structural colors, optoelectronics, as well as photoconductive devices.

CONCLUSIONS

We demonstrated a banded MV in an evaporating droplet of a PEG solution on a glass substrate. The phenomenon of particle band formation in the MV was delineated with particle dynamics associated with lateral capillary forces acting on the particles along the air−liquid interface. By conducting systematic experiments by varying the PEG concentration, particle size, and concentration, all the results were explained with a single principle: the lateral migration of particles because of CMFs acting on them along the air−liquid interface. Furthermore, a successful analogy of particle dynamics between a rotating cylinder with partially filled liquid and MV in an evaporating droplet was established.

ASSOCIATED CONTENT

Supporting Information

The Supporting Information is available free of charge on the ACS Publications website at DOI: 10.1021/acs.langmuir.9b00865.

Final particle deposition patterns on glass substrates after the complete drying of a droplet and captured images of droplets containing different particle sizes in the 0.75% PEG solution at 30 s (PDF)

Generation of a MV inside the evaporating droplet (AVI)

Banded MVs in an evaporating droplet (AVI)

Effect of the PEG concentration on the formation of banded MV in an evaporating droplet (AVI)

Effect of the particle concentration on the formation of banded MV in an evaporating droplet (AVI)

AUTHOR INFORMATION

Corresponding Author

*E-mail: lexerdshin@korea.ac.kr.

ORCID

Sehyun Shin: 0000-0002-2611-5610

Notes

The authors declare no competing financial interest.

ACKNOWLEDGMENTS

This work was supported by the National Research Foundation of Korea (NRF) Grant funded by the Korean Government (MSIP) (NRF-2016R1A5A1010148 and NRF-2015M3A9D7031026).

REFERENCES

(1) Deegan, R. D.; Bakajin, O.; Dupont, T. F.; Huber, G.; Nagel, S. R.; Witten, T. A. Capillary flow as the cause of ring stains from dried liquid drops. *Nature* **1997**, *389*, 827−829; Contact line deposit in an evaporating drop. *Phys. Rev. E: Stat. Phys., Plasmas, Fluids, Relat. Interdiscip. Top.* **2000**, *62*, 756−765.

(2) Hu, H.; Larson, R. G. Marangoni effect reverses coffee-ring depositions. *J. Phys. Chem. B* **2006**, *110*, 7090−7094.

(3) Hu, H.; Larson, R. G. Analysis of the microfluid flow in an evaporating sessile droplet. *Langmuir* **2005**, *21*, 3963−3971.

(4) Semples, W.; Dier, R. D.; Mizuno, H.; Hofkens, J.; Vermant, J. Auto-production of biosurfactants reverses the coffee ring effect in a bacterial system. *Nat. Commun.* **2013**, *4*, 1757.

(5) Ristenpart, W. D.; Kim, P. G.; Domingues, J.; Stone, H. A. Influence of substrate conductivity on circulation reversal in evaporating drops. *Phys. Rev. Lett.* **2007**, *99*, 234502.

(6) Kim, H.; Boulogne, F.; Um, E.; Jacobi, I.; Button, E.; Stone, H. A. Controlled uniform coating from the interplay of Marangoni flows and surface-adsorbed macromolecules. *Phys. Rev. Lett.* **2016**, *116*, 124501.

(7) Dan, B.; Wingfield, T. B.; Evans, J. S.; Mirri, F.; Pint, C. L.; Pasquali, M.; Smalyukh, I. I. Templating of self-alignment patterns of anisotropic gold nanoparticles on ordered SWNT macrostructures. *ACS Appl. Mater. Interfaces* **2011**, *3*, 3718−3724.

(8) Naqshbandi, M.; Canning, J.; Gibson, B. C.; Nash, M. M.; Crossley, M. J. Room temperature self-assembly of mixed nanoparticles into photonic structures. *Nat. Commun.Nat. Comm.* **2012**, *3*, 1188.

(9) Jing, J.; Reed, J.; Huang, J.; Hu, X.; Clarke, V.; Edington, J.; Housman, D.; Anantharaman, T. S.; Huff, E. J.; Mishra, B.; Porter, B.; Shenker, Al.; Wolfson, E.; Hiort, C.; Kantor, R.; Aston, C.; Schwartz, D. C. Automated high-resolution optical mapping using arrayed fluid-fixed DNA molecules. *Proc. Natl. Acad. Sci. U.S.A.* **1998**, *95*, 8046−8051.

(10) Park, J.; Moon, J. Control of colloidal particle deposit patterns within picoliter droplets ejected by ink-jet printing. *Langmuir* **2006**, *22*, 3506−3513.

(11) Kuang, M.; Wang, L.; Song, Y. Controllable printing droplets for high-resolution patterns. *Adv. Mater.* **2014**, *26*, 6950−6958.

DOI: 10.1021/acs.langmuir.9b00865
Langmuir 2019, 35, 8977−8983

(12) Zhang, X.; Wang, J.; Bao, L.; Dietrich, E.; van der Veen, R. C. A.; Peng, S.; Friend, J.; Zandvliet, H. J. W.; Yeo, L.; Lohse, D. Mixed mode of dissolving immersed nanodroplets at a solid-water interface. *Soft Matter* **2015**, *11*, 1889−1900.
(13) Chhasatia, V. H.; Joshi, A. S.; Sun, Y. Effect of relative humidity on contact angle and particle deposition morphology of an evaporating colloidal drop. *Appl. Phys. Lett.* **2010**, *97*, 231909.
(14) Li, Y.; Yang, Q.; Li, M.; Song, Y. Rate-dependent interface capture beyond the coffee-ring effect. *Sci. Rep.* **2016**, *6*, 24628.
(15) Bhardwaj, R.; Fang, X.; Somasundaran, P.; Attinger, D. Self-assembly of colloidal particles from evaporating droplets: role of DLVO interactions and proposition of a phase diagram. *Langmuir* **2010**, *26*, 7833−7842.
(16) Bigioni, T. P.; Lin, X.-M.; Nguyen, T. T.; Corwin, E. I.; Witten, T. A.; Jaeger, H. M. Kinetically driven self assembly of highly ordered nanoparticle monolayers. *Nat. Mater.* **2006**, *5*, 265−270.
(17) Marín, Á. G.; Gelderblom, H.; Lohse, D.; Snoeijer, J. H. Order-to-disorder transition in ring-shaped colloidal stains. *Phys. Rev. Lett.* **2011**, *107*, 085502.
(18) Seo, C.; Jang, D.; Chae, J.; Shin, S. Altering the coffee-ring effect by adding a surfactant-like viscous polymer solution. *Sci. Rep.* **2017**, *7*, 500.
(19) Yunker, P. J.; Still, T.; Lohr, M. A.; Yodh, A. G. Suppression of the coffee-ring effect by shape-dependent capillary interactions. *Nature* **2011**, *476*, 308.
(20) Loudet, J. C.; Alsayed, A. M.; Zhang, J.; Yodh, A. G. Capillary interactions between anisotropic colloidal particles. *Phys. Rev. Lett.* **2005**, *94*, 018301.
(21) Sefiane, K. Internal fluid motion and particle transport in externally heated sessile droplets. *J. Bionic Eng.* **2010**, *7*, 82−93.
(22) Thokchom, A. K.; Majumder, S. K.; Singh, A. Internal fluid motion and particle transport in externally heated sessile droplets. *AIChE J.* **2016**, *62*, 1308−1321.
(23) Anyfantakis, M.; Baigl, D. Manipulating the Coffee-Ring Effect: Interactions at Work. *ChemPhysChem* **2015**, *16*, 2726−2734.
(24) Shmuylovich, L.; Shen, A. Q.; Stone, H. A. Surface morphology of drying latex films: Multiple ring formation. *Langmuir* **2002**, *18*, 3442−3445.
(25) Yang, X.; Li, C. Y.; Sun, Y. From multi-ring to spider web and radial spoke: competition between the receding contact line and particle deposition in a drying colloidal drop. *Soft Matter* **2014**, *10*, 4458−4463.
(26) Weon, B. K.; Je, J. H. Fingering inside the coffee ring. *Phys. Rev. E: Stat., Nonlinear, Soft Matter Phys.* **2013**, *87*, 013003.
(27) Senses, E.; Black, M.; Cunningham, T.; Sukhishvili, S. A.; Akcora, P. Spatial ordering of colloids in a drying aqueous polymer droplet. *Langmuir* **2013**, *29*, 2588−2594.
(28) Kralchevskyt, P. A.; Paunov, V. N.; Nagayama, K. Capillary meniscus interaction between colloidal particles attached to a liquid—fluid interface. *J. Colloid Interface Sci.* **1992**, *151*, 79−94.
(29) Danov, N. D. Two-dimensional crystallization. *Nature* **1993**, *361*, 26.
(30) Kralchevsky, P. A.; Nagayama, K. Capillary forces between colloidal particles. *Langmuir* **1994**, *10*, 23−36.
(31) Danov, K. D.; Pouligny, B.; Kralchevsky, P. A. Capillary Forces between Colloidal Particles Confined in a Liquid Film: The Finite-Meniscus Problem. *Langmuir* **2001**, *17*, 6599−6609.
(32) Tirumkudulu, M.; Tripathi, A.; Acrivos, A. Particle segregation in monodisperse sheared suspensions. *Phys. Fluids* **1999**, *11*, 507−509.
(33) Timberlake, B. D.; Morris, J. F. Concentration band dynamics in free-surface Couette flow of a suspension. *Phys. Fluids* **2002**, *14*, 1580−1589.
(34) Joseph, D. D.; Wang, J.; Bai, R.; Yang, B. H.; Hu, H. H. Particle motion in a liquid film rimming the inside of a partially filled rotating cylinder. *J. Fluid Mech.* **2003**, *496*, 139−163.
(35) Maisel, K.; Reddy, M.; Xu, Q.; Chattopadhyay, S.; Cone, R.; Ensign, L. M.; Hanes, J. Nanoparticles coated with high molecular weight PEG penetrate mucus and provide uniform vaginal and colorectal distribution in vivo. *Nanomedicine* **2016**, *11*, 1337−1343.
(36) Bowden, N.; Arias, F.; Deng, T.; Whitesides, G. W. Self-assembly of microscale objects at a liquid/liquid interface through lateral capillary forces. *Langmuir* **2001**, *17*, 1757−1765.

DOI: 10.1021/acs.langmuir.9b00865
Langmuir 2019, 35, 8977−8983